

Supporting Information

Nitrogen-doped graphene for dye-sensitized solar cells and the role of nitrogen states in triiodide reduction

Shaocong Hou, Xin Cai, Hongwei Wu, Xiao Yu, Ming Peng, Kai Yan, Dechun Zou*

Beijing National Laboratory for Molecular Sciences, Key Laboratory of Polymer Chemistry and Physics of Ministry of Education, College of Chemistry and Molecular Engineering, Peking University, Beijing 100871, China.

E-mail: dczou@pku.edu.cn

Experimental detail

Characterization of GO/cyanamide. Thermal properties of GO/Cyanamide composites were studied with simultaneous TGA-DTA-DSC thermal analyzer (SDT Q600) at a heating rate of 5 K/min from room temperature to 1000°C.

Characterization of NrG. XRD was carried out on DMAX-2400 (Rigaku, Japan). Raman spectra was measured by Raman Imaging Microscope System (Renishaw 1000) with a excitation wavelength of 632.8 nm.

Electrochemical testing. All electrochemical characterization in supporting information were carried out on Electrochemical Workstation (Autolab PG320) with three-electrode cell, where Ag/Ag⁺ and Pt wire was used as reference electrode and auxiliary electrode, respectively. Ti wire loaded with 10 μg NrG was used as the working electrode. For electroactive area measurement, cyclic voltammetry was performed in the acetonitrile solution containing 1 mM Ferrocene and 0.1 M LiClO₄ at the scanning rate of 0.1V/s from -0.5V to 0.5V. For electrocatalytic activity measurement, the acetonitrile-based electrolyte contains 3 mM I₂, 60 mM DMII, 0.1 M LiClO₄.

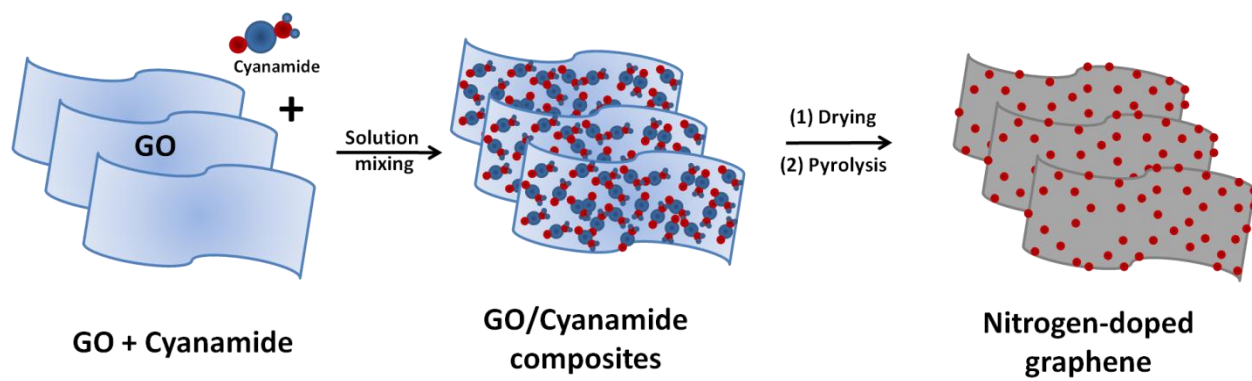


Fig. S1. Scheme of the fabrication process of nitrogen-doped graphene (NrG).

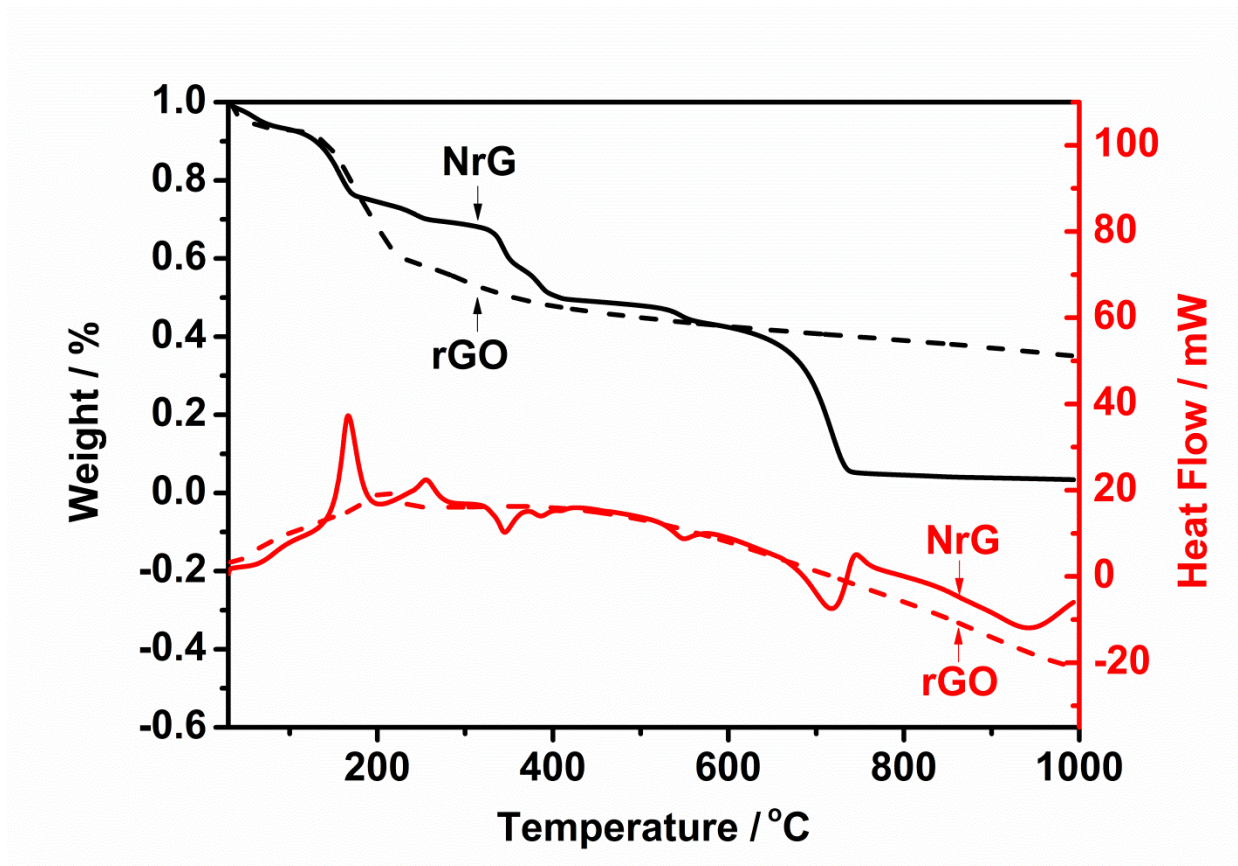


Fig. S2. Thermal properties of the GO/Cyanamide composites (NrG) and pure graphene oxide (rGO).

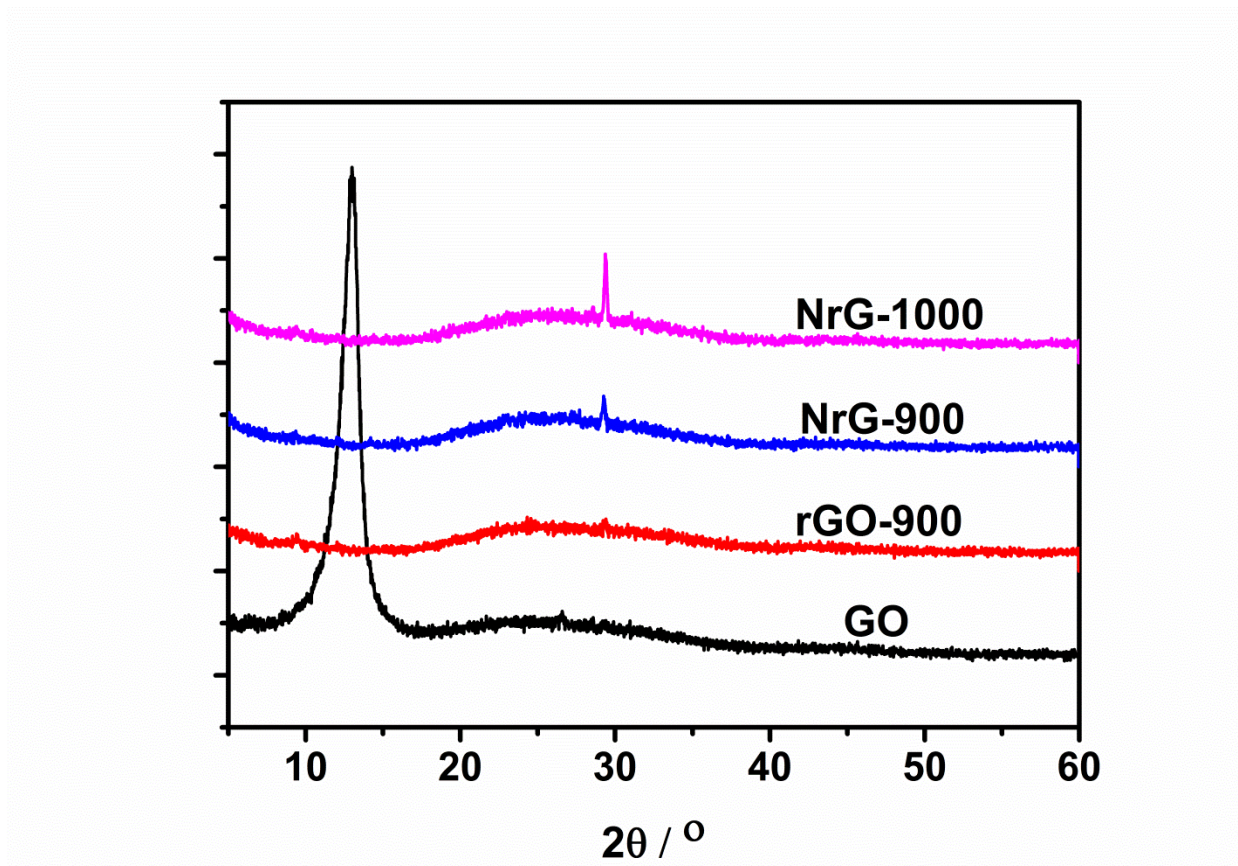


Fig. S3. XRD of GO, rGO-900, NrG-900, and NrG-10000.

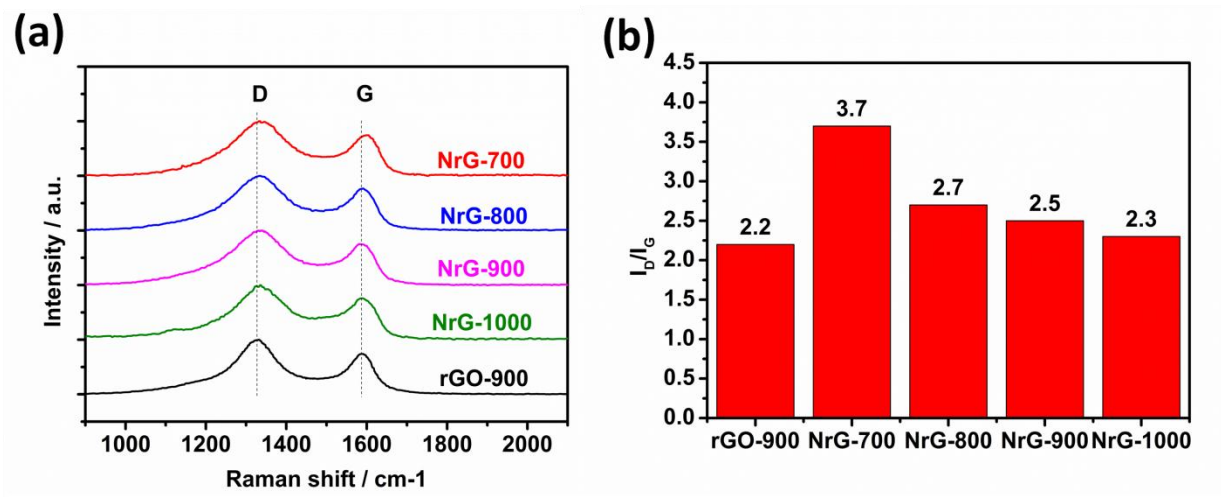


Fig. S4. Raman spectra of rGO-900, NrG-700, NrG-800, NrG-900, and NrG-10000.

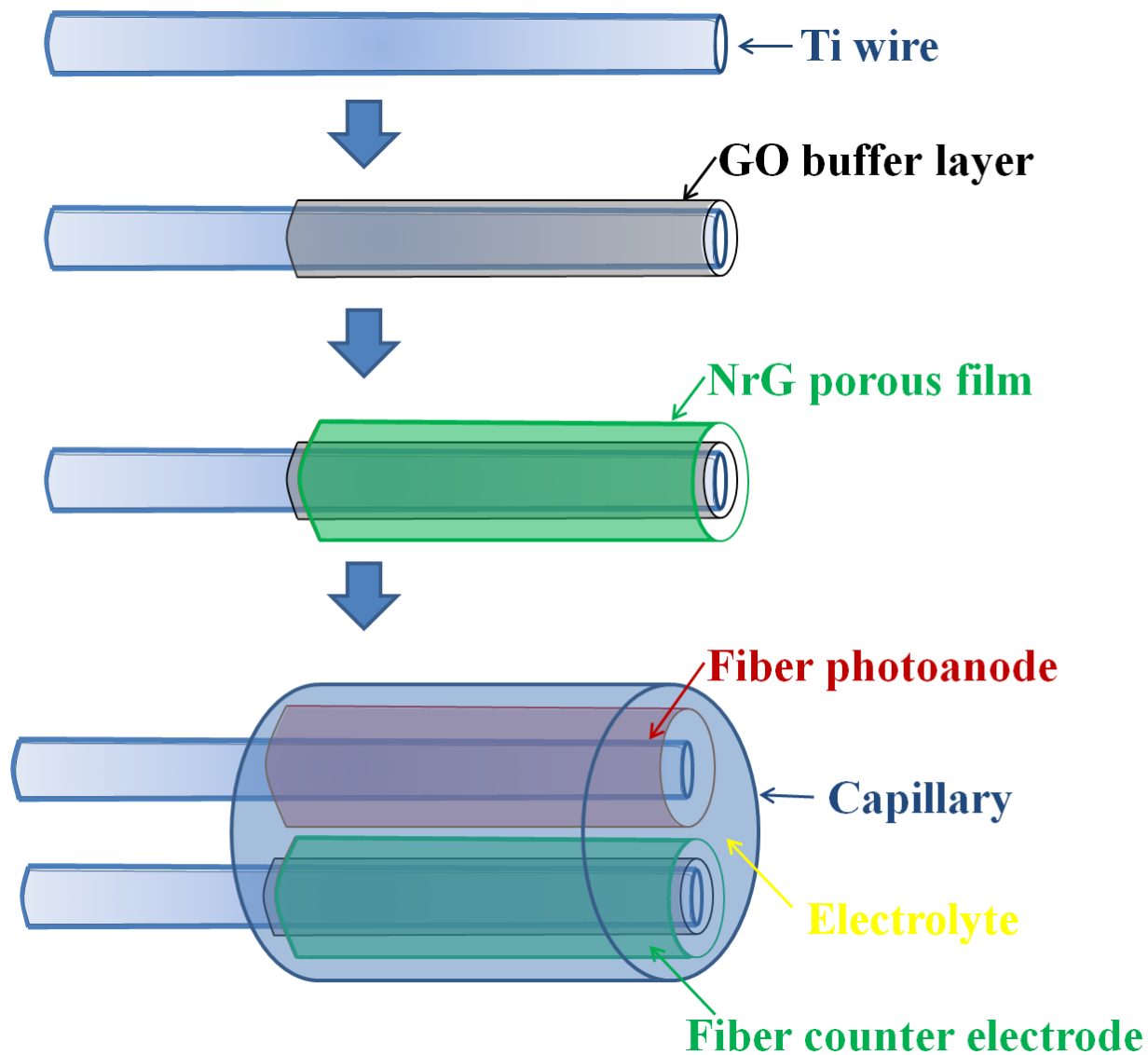


Fig. S5. Scheme of the fabrication process of the graphene-based fiber counter electrode and fiber solar cell.

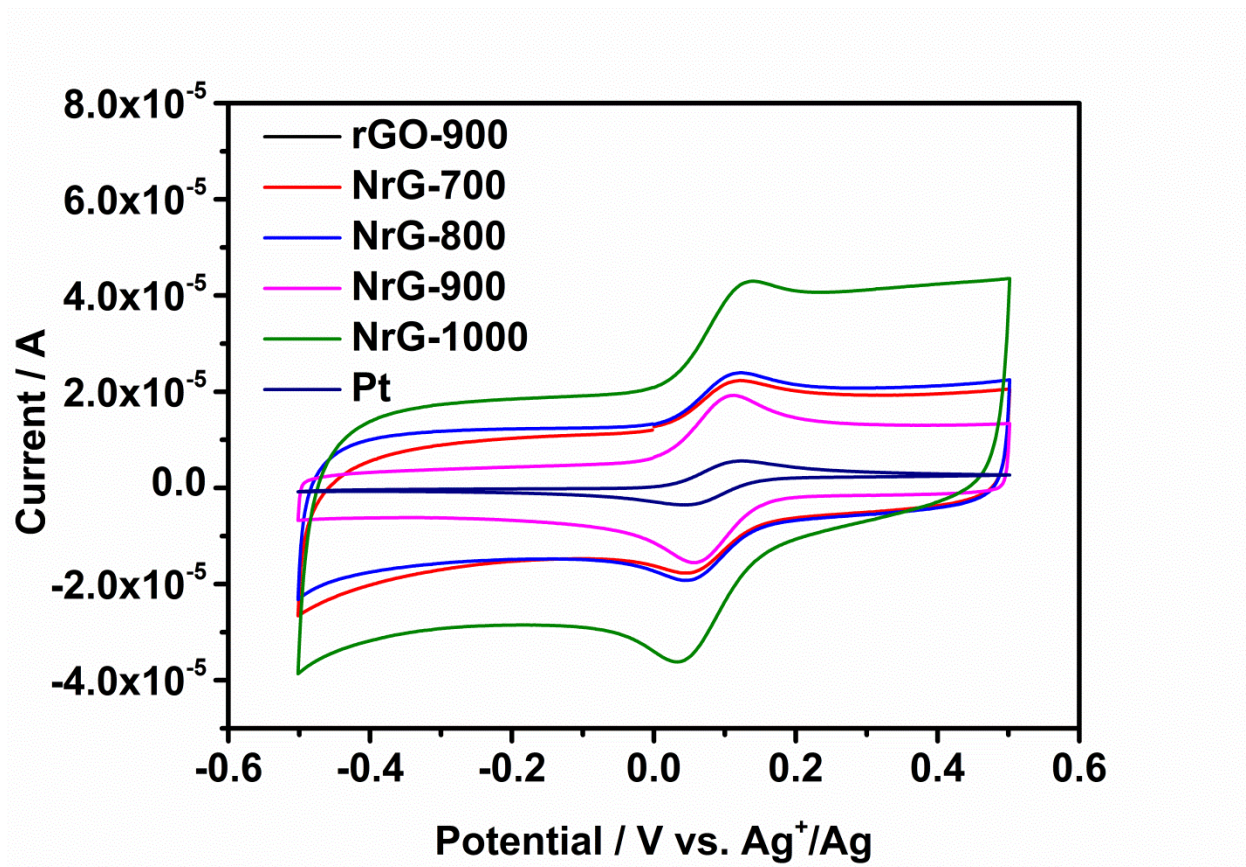


Fig. S6. CV of different electrocatalysts in acetonitrile solution of ferrocene.

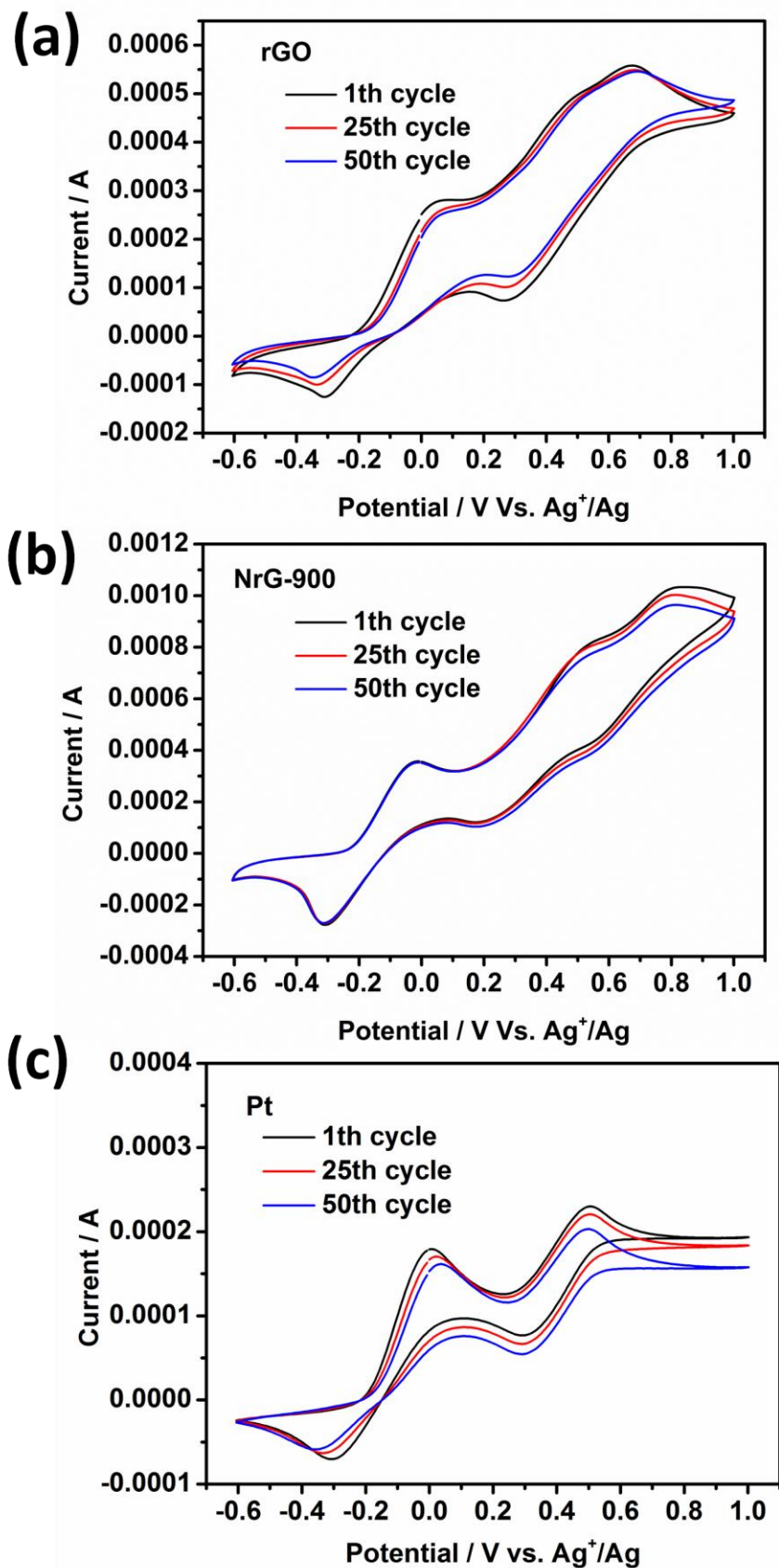


Fig. S7. Continuous CV of rGO (a), NrG-900 (b) and Pt (c) in I_3^-/I^- electrolytes at a scanning rate of 0.1 V/s from -0.6 V to 1.0 V.

Similar to Pt electrocatalyst, pristine graphene (rGO) shows two couples of redox peaks in CV curve (Fig. S7a), which correspond to I_3^-/I^- and I_2/I_3^- redox reaction, respectively. (S. C. Hou, *et al.*, *Journal of Power Sources* 2012, 215, 164-169) Compared with Pt and rGO, nitrogen-doped graphene (NrG-900) also shows two couples of redox peaks corresponding to I_3^-/I^- and I_2/I_3^- redox reaction. Notably, a new couple of redox peaks emerges in the right side of CV curve. Although the original of the third pair of peaks is still unclear, but it is probably caused by nitrogen-containing functional groups in graphene. J. D. Roy-Mayhew also found the third pair of peaks in CV curves of oxygen-doped graphene, and they speculated it originated from oxygen-containing functional groups in graphene. (J. D. Roy-Mayhew, *et al.*, *Acs Nano*, 2010, 4, 6203.)

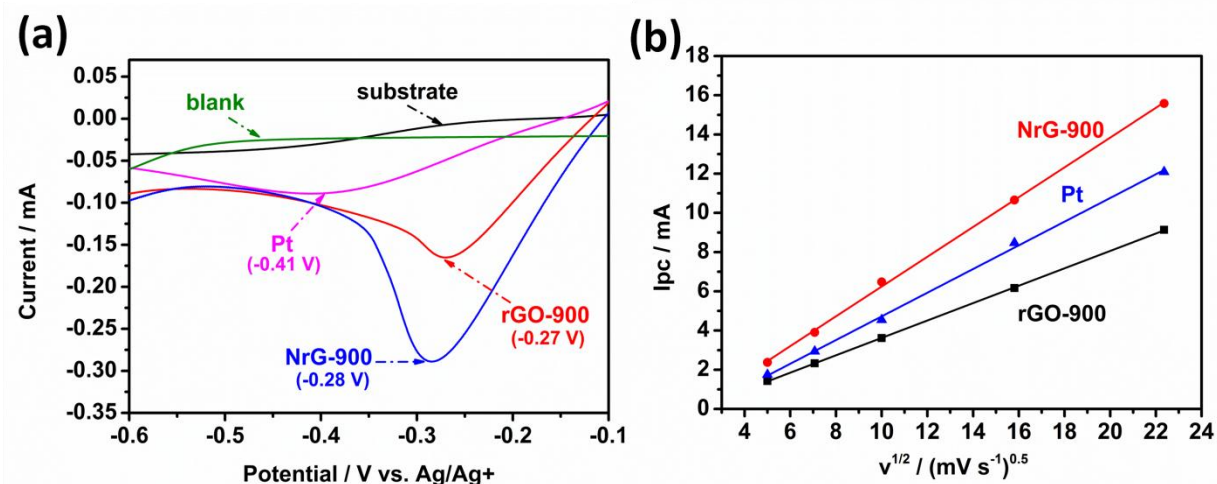


Fig. S8. Linear sweep voltammetry of different electrocatalysts in I_3^-/I^- electrolyte at scanning rate of 0.1 V/s from 0 V to -0.6 V and the relationships between the cathode peak current and the scanning rates. The substrate or blank denoted the unmodified or GO-modified Ti wire, respectively.

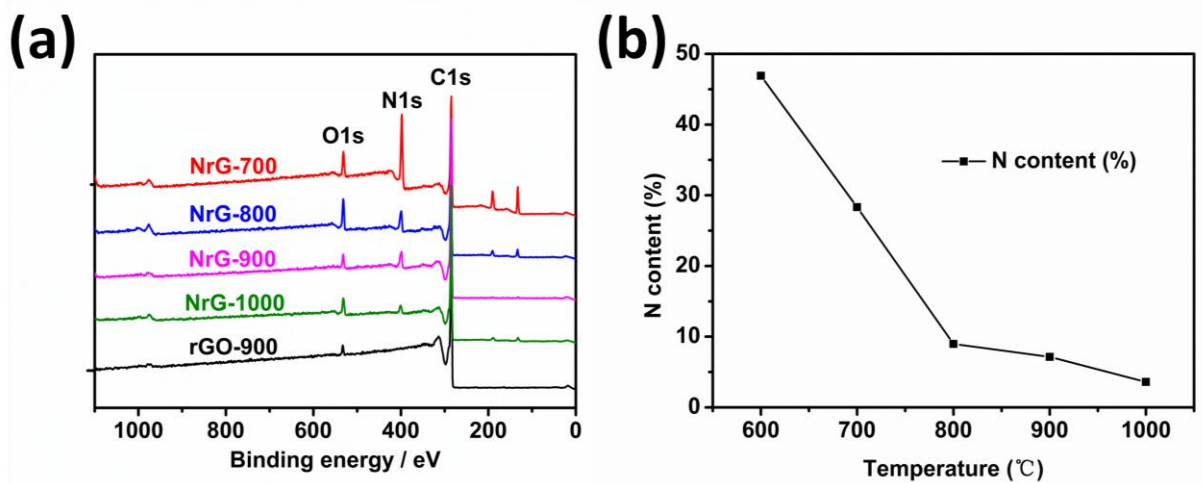


Fig. S9. XPS spectra (a) and N content (b) of NrG-700, NrG-800, NrG-900, and NrG-1000.

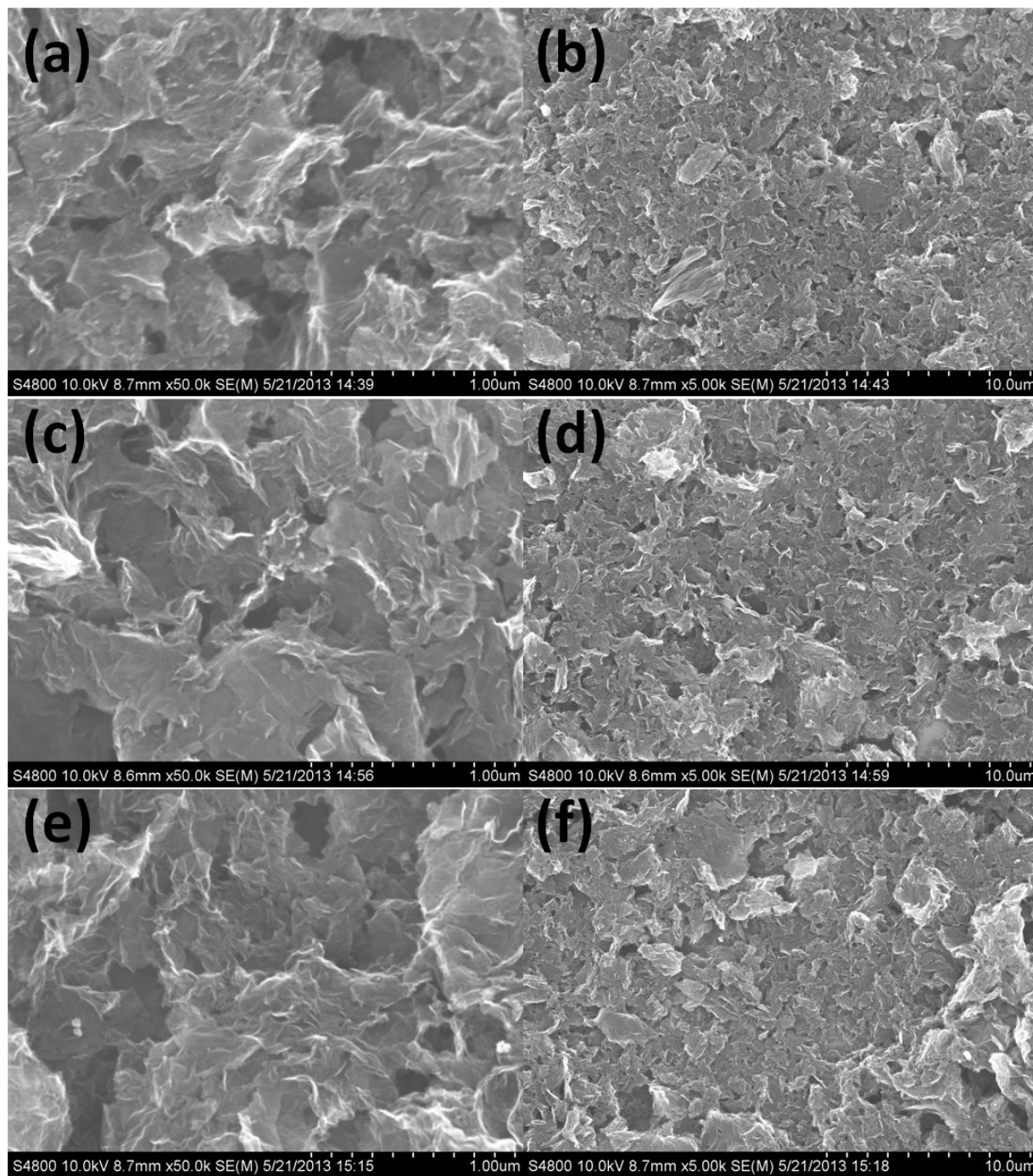


Fig. S10. SEM of NrG-700(a, b), NrG-800(c, d) and NrG-1000(e, f).

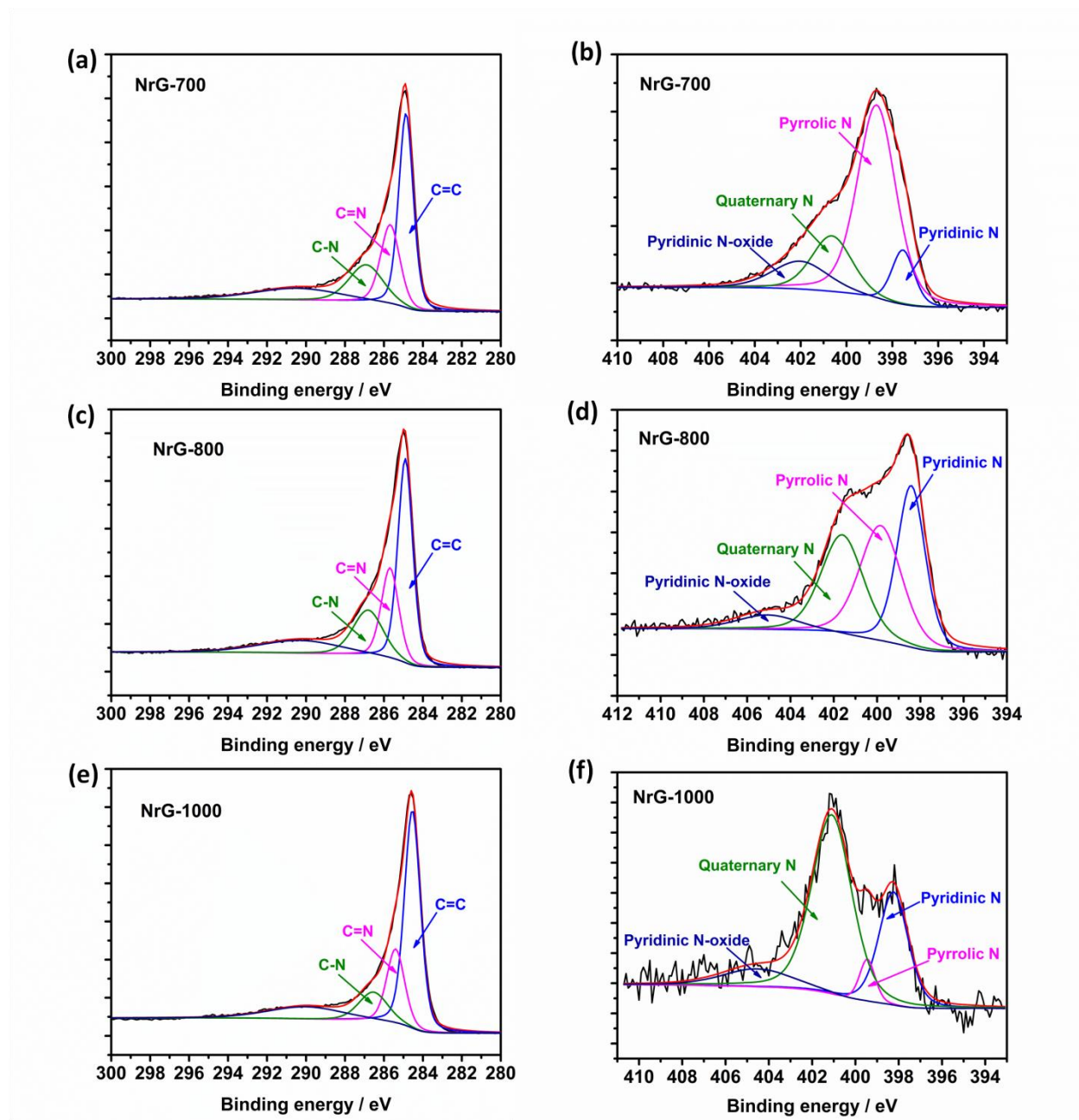


Fig. S11. High resolution C1s XPS spectra of NrG-700(a), NrG-800(c) and NrG-1000(e) and high resolution N1s XPS spectra of NrG-700(b), NrG-800(d) and NrG-1000(f)

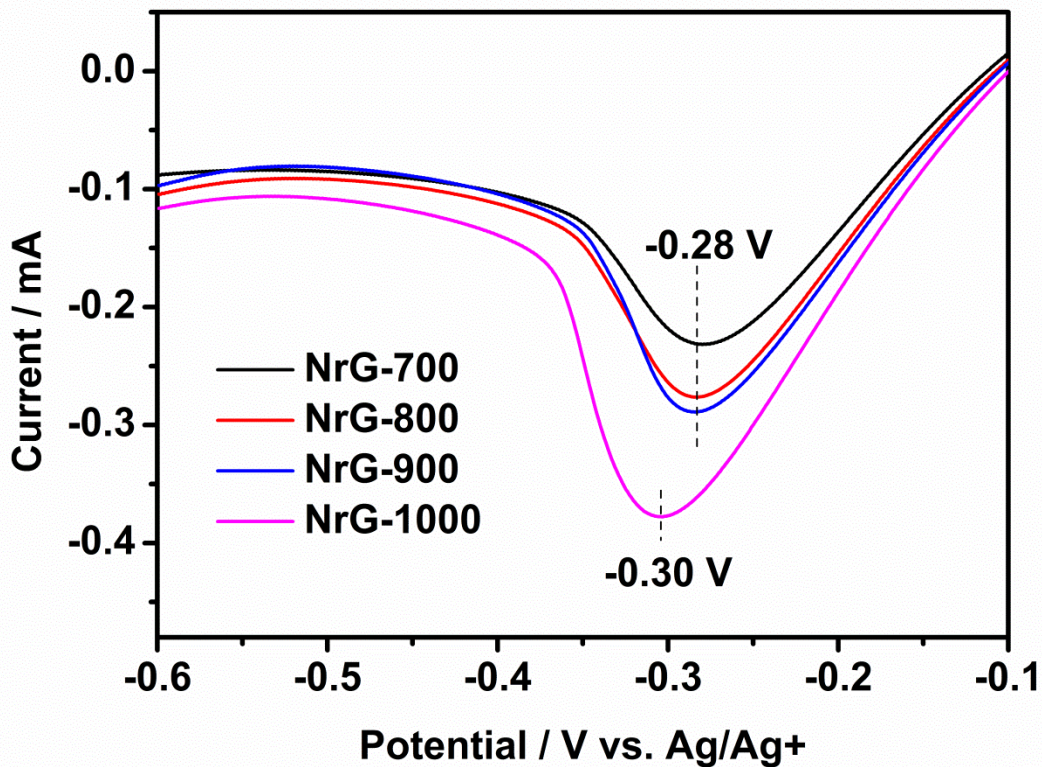


Fig. S12. LSV of different electrocatalysts in I_3^-/I^- electrolytes and the relationships between the cathode peak current and the scanning rates.

Table S1. CV of different electrocatalysts in acetonitrile solution of ferrocene.

Electrocatalysts	$E_{\text{Fc/Fc}^+}$ / mV	I_{pa} / μA	β	$J_0'/J_{0,\text{Pt}}$
rGO-900	84	13.1	2.3	0.13
NrG-700	84	8.76	1.6	0.26
NrG-800	85	10.4	1.9	0.59
NrG-900	84	1.14	2.1	0.67
NrG-1000	87	21.7	3.9	0.14
Pt	82	5.55	1.0	1

Note:a) The electroactive surface area (A_{eff}) was calculated with Randles-Sevcik equation, and $\beta = A_{\text{eff}}/A_{\text{eff,Pt}}$, where $A_{\text{eff,Pt}}$ is the electroactive surface area of Pt electrocatalyst.

b) The intrinsic exchange current, $J_0' = J_0/\beta = RT/(nF\beta R_{\text{ct}})$.

Table S2 The composition atomic ratios of each type of N species in four NrG samples

Electrocatalysts	C (at.%)	N (at.%)	Pyridinic N (at.%)	Quaternary N (at.%)	PyrrolicN (at.%)	Pyridinic N-oxide (at.%)
NrG-700	72.2	18	1.78	3.26	10.7	2.25
NrG-800	80.4	9.5	2.96	2.73	3.15	0.61
NrG-900	89.2	7.4	2.99	3.33	0.39	0.64
NrG-1000	90.4	3.6	0.95	2.04	0.19	0.36

Table S3 Comparison of our work with others' studies on nitrogen-doped graphene for dye-sensitized solar cells in literature.

	Method	Precursors	O content	N content	N states	Reference ^[b]
1	Hydrothermal	GO+NH ₃	N.A. ^[a]	2.5%	pyridinic:pyrrolic	[1]
2	Hydrothermal	GO+NH ₃	N.A. ^[a]	2.5%	N.A.	[2]
3	Hydrothermal	GO+N ₂ H ₄ +N H ₃	N.A. ^[a]	NA	pyridinic: pyrrolic:graphitic	[3]
4	Annealing	4-aminobenzoyl functionalized graphene	N.A. ^[a]	2.79%	N.A.	[4]
5	Annealing	GO+NH ₃	N.A. ^[a]	7.6%	pyridinic:pyrrolic	[5]
6	Annealing	GO+NH ₃	~7.5%	1.71- 4.14%	pyridinic:pyrolic:graphitic	[6]
This work	Annealing	GO+ Cyanamide	3.3- 7.8%	3.6- 18%	pyridinic:pyrrolic:quaternar y:N-oxide of pyridinic	

^[a]The exact oxygen content of nitrogen-doped graphene is not given, but higher content of oxygen than that nitrogen could be easily found in XPS spectra in the corresponding paper.

^[b]Reference:

1. G. Q. Wang, Y. Y. Fang, Y. Lin, W. Xing and S. P. Zhuo, *Mater Res Bull*, 2012, **47**, 4252-4256.
2. G. Q. Wang, W. Xing and S. P. Zhuo, *Electrochimica Acta*, 2013, **92**, 269-275.
3. M. Y. Yen, C. K. Hsieh, C. C. Teng, M. C. Hsiao, P. I. Liu, C. C. M. Ma, M. C. Tsai, C. H. Tsai, Y. R. Lin and T. Y. Chou, *Rsc Advances*, 2012, **2**, 2725-2728.
4. M. J. Ju, J. C. Kim, H. J. Choi, I. T. Choi, S. G. Kim, K. Lim, J. Ko, J. J. Lee, I. Y. Jeon, J. B. Baek and H. K. Kim, *Acs Nano*, 2013, **7**, 5243-5250.
5. Y. Xue, J. Liu, H. Chen, R. Wang, D. Li, J. Qu and L. Dai, *Angewandte Chemie*, 2012, **51**, 12124-12127.
6. X. Y. Zhang, S. P. Pang, X. Chen, K. J. Zhang, Z. H. Liu, X. H. Zhou and G. L. Cui, *Rsc Advances*, 2013, **3**, 9005-9010.